Received: 13 December 2021 | Revised: 24 February 2022 | Accepted: 26 February 2022

DOI: 10.1002/jcla.24401

RESEARCH ARTICLE

WILEY

Hsa_circ_0058129 regulates papillary thyroid cancer development via miR-873-5p/follistatin-like 1 axis

Xiangrong Tan | Jiazheng Zhao | Jianlin Lou | Wen Zheng | Peng Wang

Head and Neck Surgery, The Cancer Hospital of the University of Chinese Academy of Sciences (Zhejiang Cancer Hospital), Institute of Basic Medicine and Cancer (IBMC), Chinese Academy of Sciences, Hangzhou, China

Correspondence
Xiangrong Tan, No.1, Banshan East Road, Hangzhou, Zhejiang Province 310022, China.
Email: tanxr@zjcc.org.cn

Abstract

Background: Papillary thyroid cancer (PTC) is an endocrine malignancy with a high incidence. Circular RNAs (circRNAs) participate in regulating PTC. Here, we analyzed the role of hsa_circ_0058129 (circ_0058129) in PTC.

Methods: The expression of circ_0058129, fibronectin 1 (FN1) mRNA, microRNA-873-5p (miR-873-5p), and follistatin-like 1 (FSTL1) was detected by qRT-PCR and western blot. Cell proliferation was analyzed by CCK-8, EdU, and flow cytometry analysis assays. Cell migration and invasion were evaluated by Transwell assay. The targeting relationship of miR-873-5p and circ_0058129 or FSTL1 was identified through dual-luciferase reporter assay, RIP assay, and RNA pull-down assay. Xenograft mouse model assay was implemented to determine the effect of circ_0058129 on tumor formation in vivo.

Results: The circ_0058129 and FSTL1 abundances were increased, while the miR-873-5p content was decreased in PTC tissues and cells compared with control groups. Circ_0058129 shortage inhibited PTC cell proliferation, migration, and invasion. Moreover, miR-873-5p repressed PTC cell malignancy by binding to FSTL1. Circ_0058129 targeted miR-873-5p to regulate FSTL1.

Conclusion: Circ_0058129 expedited PTC progression through the miR-873-5p/FSTL1 pathway.

KEYWORDS
FSTL1, hsa_circ_0058129, miR-873-5p, papillary thyroid cancer

1 | INTRODUCTION

Papillary thyroid cancer (PTC) accounts for about 80% of all thyroid cancers.[1] People aged 30–50 are susceptible to PTC, and the incidence gradually increases with age.[2] Currently, the main therapeutic methods for PTC are surgical resection, thyroid hormone suppression, and radioactive iodine therapy. More than 25% of PTC patients relapse, and the etiology is complex and still unclear.[3] Therefore, developing novel treatment strategies is necessary to improve the poor outcome.

Circular RNAs (circRNAs) are a type of RNAs and participate in the progression of several cancers.[4,5] For instance, hsa_circ_102171 promoted PTC progression.[6] Hsa_circ_0137287 suppressed PTC development.[7] Besides, hsa_circ_0006156 acted as a new marker for PTC diagnosis.[8] In particular, Yao et al.[9] reported that the abundance of circ_0058124, circ_0058129, and circ_0060983 was boosted

in PTC and invasive PTC. Circ_0058124 has been investigated by Yao and his colleagues, and their results showed that the circRNA contributes to PTC cell malignancy.[9] Additionally, previous data explained that the parental gene of circ_0058129, fibronectin 1 (FN1), participated in thyroid cancer progression.[10] Nevertheless, the function of circ_0058129 in PTC has not been studied yet.

MicroRNAs (miRNAs) are a kind of RNAs that can modulate cell functions by combining with genes.[11,12] For example, miR-873-5p impeded the advancement of colon cancer.[13] MiR-873-5p inhibited PTC cell migration.[14] Besides, miR-873-5p regulated gastric cancer development.[15] MiR-145 could regulate the cell proliferation of PTC.[16] MiR-148a inhibited cell growth of PTC.[17] Nevertheless, the influence of miR-873-5p on PTC progression remains to be explored.

Follistatin-like 1 (FSTL1) is a cysteine-rich secretory glycoprotein.[18] FSTL1 serves as a key participant in physiological developments, such as growth, immune regulation, and differentiation.[19,20] Meanwhile, FSTL1 regulates breast cancer cell growth.[21] In addition, FSTL1 overturned cell invasion in non-small cell lung cancer.[22] Nevertheless, there are little data on the effect of FSTL1 in PTC.

Herein, we hypothesized that circ_0058129 could regulate tumor growth of PTC by interacting with miR-873-5p and FSTL1. We investigated the role of circ_0058129 in PTC cell malignancy, and determined whether miR-873-5p and FSTL1 were involved in the mechanism responsible for circ_0058129-mediated PTC progression with the hope of providing therapeutic targets for PTC.

2 | MATERIALS AND METHODS

2.1 | Clinical samples

The study was approved by the Ethics Committee of the Cancer Hospital of the University of Chinese Academy of Sciences. Seventy pairs of PTC tissues and paracarcinoma tissues were congregated from the Cancer Hospital of the University of Chinese Academy of Sciences. All participants offered the informed consent.

2.2 | Cell lines

Papillary thyroid cancer cell lines (TPC-1 and SNU-790) and Nthy-ori 3–1 cells were procured from Cell Bank, Chinese Academy of Sciences (CAS). These cells were cultivated in RPMI-1640 medium in an incubator with 5% CO_2.

2.3 | QRT-PCR and RNase R assay

RNAs were prepared using Trizol (Sigma-Aldrich). RNase R was utilized to identify the stability of circ_0058129 and FN1 mRNA. Two micrograms of RNA was hatched with or without RNase R (3 U/μg, TaKaRa) for 30 min. To detect the contents of circ_0058129 and mRNA, cDNA was produced utilizing PrimeScript RT Reagent Kit (TaKaRa). For miRNA, cDNA was prepared using miR First-Strand Synthesis Kit (TaKaRa). The qRT-PCR was performed by SYBR Premix Ex Taq II (TaKaRa) and SYBR Green kit (Sigma). GAPDH and RNU6 (U6) served as internal controls. The primers are listed in Table 1.

TABLE 1 Primers for PCR

Name		Primers for PCR (5′-3′)
hsa_circ_0058129	Forward	TCAAGAAAGTACACCTGTTGTCA
	Reverse	ACCACCAGTCTCATGTGGTC
FN1	Forward	ACAAGCATGTCTCTCTGCCA
	Reverse	TTTGCATCTTGGTTGGCTGC
miR-873-5p	Forward	GCCGAGGCAGGAACTTGTG
	Reverse	GTGCGTGTCGTGGAGTCG
FSTL1	Forward	CCACGTGGACCAGTCTGAAT
	Reverse	GGCCTTAATTGGGGGAAAGGA
U6	Forward	CTTCGGCAGCACATATACT
	Reverse	ACGCTTCACGAATTTGCGTGTC
GAPDH	Forward	TCCCATCACCATCTTCCAGG
	Reverse	GATGACCCTTTTGGCTCCC

2.4 | Subcellular fractionation location assay

SNU-790 and TPC-1 cells were harvested and incubated with CEB-A Mix and ice-cold Cytosol Extraction Buffer-B as per the guidebook of Nuclear/Cytosol Fractionation Kit (Amyjet). Then, the supernatant was transferred to prechilled tubes. At last, the supernatants containing cytoplasmic extract and the pellets (containing nuclei) were lysed, and qRT-PCR was used to analyze circ_0058129 expression.

2.5 | Western blot

The proteins were prepared by the Protein Extraction Kit (Sigma). The 30–40 μg protein was separated by 12% SDS-PAGE gels and transferred onto PVDF membranes (Sigma). After blocking, the membranes were exposed to the following antibodies: anti-FSTL1 (ab223287; 1:1000; Abcam), anti-E-cadherin (ab40772; 1:10,000; Abcam), anti-N-cadherin (ab76011; 1:1,000; Abcam), anti-Vimentin (ab92547; 1:1,000; Abcam), and anti-GAPDH (ab9485; 1:2500; Abcam). After being incubated with secondary antibodies (ab205718; 1:2500; Abcam), the membranes were evaluated.

2.6 | Cell transfection

The small RNAs of circ_0058129 (si-circ_0058129#1, si-circ_0058129#2, sh-circ_0058129), the controls (si-NC and sh-NC), miR-873-5p mimics, miR-873-5p inhibitors, controls, FSTL1, and

pcDNA were attained from Ribobio. Transfection was carried out using Lipofectamine 2000 (Sigma).

2.7 | Cell proliferation assay

After transfection, PTC cells (2.0×10^3/well) were plated in 96-well plates. CCK-8 (Sigma) was used to incubate the cells in accordance with the commands. Besides, the Cell-Light™ EdU kit (Sigma) was implemented to evaluate cell proliferation. In simple terms, PTC cells with transfection (6.0×10^4/well) were seeded in 24-well plates and incubated with EdU (50 μM) for 2 h. The cells were exposed to 4% formaldehyde for 0.5 h and hatched with 2 mg/ml glycine for 10 min. The cells were exposed to Apollo solution (Sigma) and DAPI (Sigma). Lastly, the images were achieved by microscopy.

2.8 | Flow cytometry assay

Papillary thyroid cancer (1×10^6) cells were cultivated in six-well plates. A PI Flow Cytometry Kit (Abcam) was utilized to assess PTC cells, referring to the procedure. The cells were exposed to 75% ethanol and treated with PI for 0.5 h. These cells were evaluated by flow cytometry.

2.9 | Transwell assay

Papillary thyroid cancer cells were assessed by a transwell with polycarbonate membrane (8 μm pore; BD Bio-sciences). In brief, 4×10^5 transfected PTC cells, suspended in 100 μl DMEM deprived of serum, were planted into the top chamber. Then, the inferior chamber of the transwell was added with 500 μl of DMEM and 10% FBS. Next, the cells on the inferior membrane were stained, and cell migratory ability was analyzed under a microscope. The equivalent model was used to detect cell invasive ability with the chamber pre-coated with matrigel (BD Biosciences).

2.10 | Dual-luciferase reporter assay

The combinative sequence of miR-873-5p and circ_0058129 or FSTL1 was predicted by circinteractome and targetscan. Then,

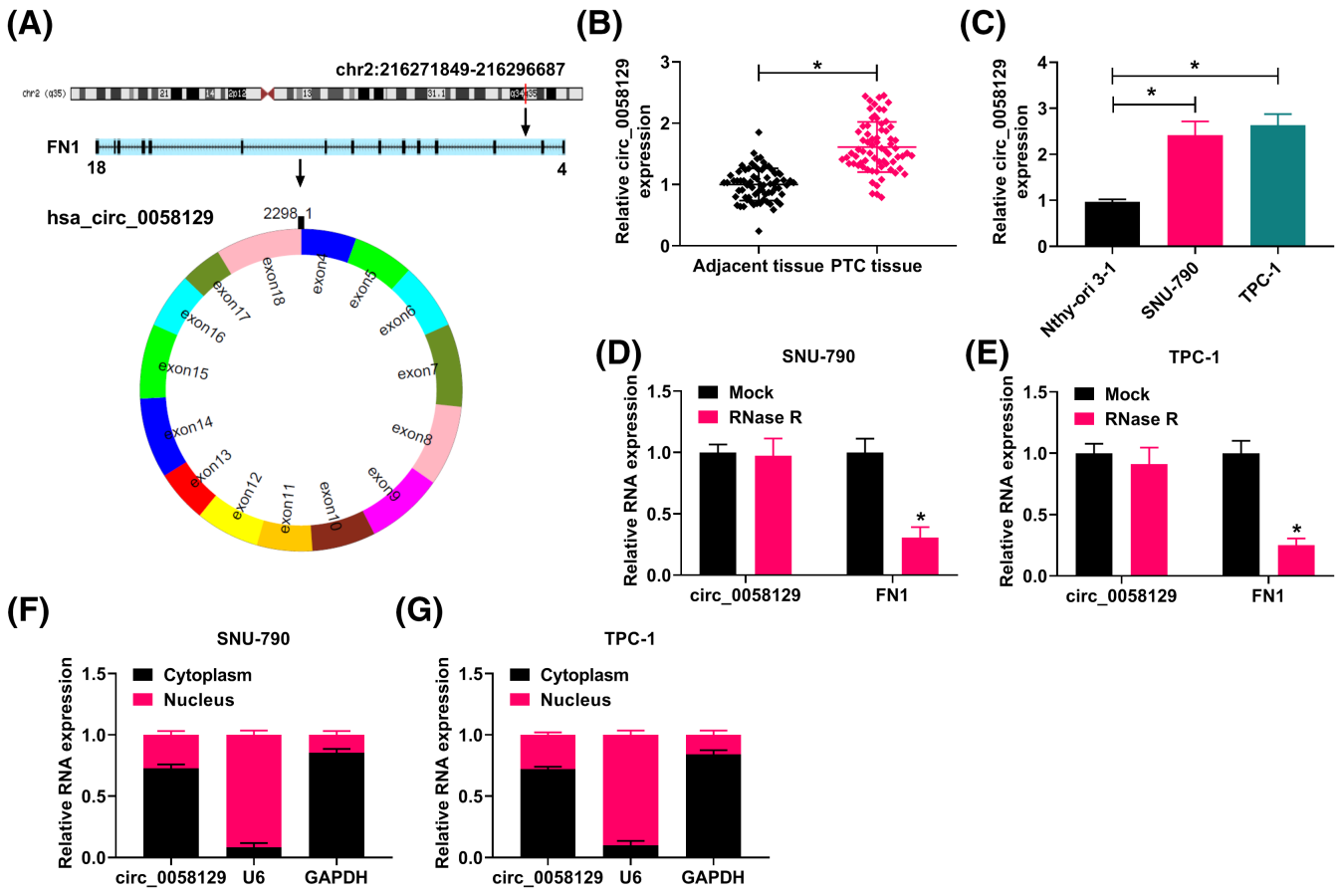

FIGURE 1 Circ_0058129 was enhanced in PTC tissues. (A) The schematic illustration showed the generation of circ_0058129. (B and C) The abundance of circ_0058129 was detected by qRT-PCR. (D and E) RNase R treatment assay analyzed the circular structure of circ_0058129. (F and G) Subcellular fractionation location assay demonstrated that circ_0058129 was mainly located in the cytoplasm of SUN-790 and TPC-1 cells. *$p < 0.05$

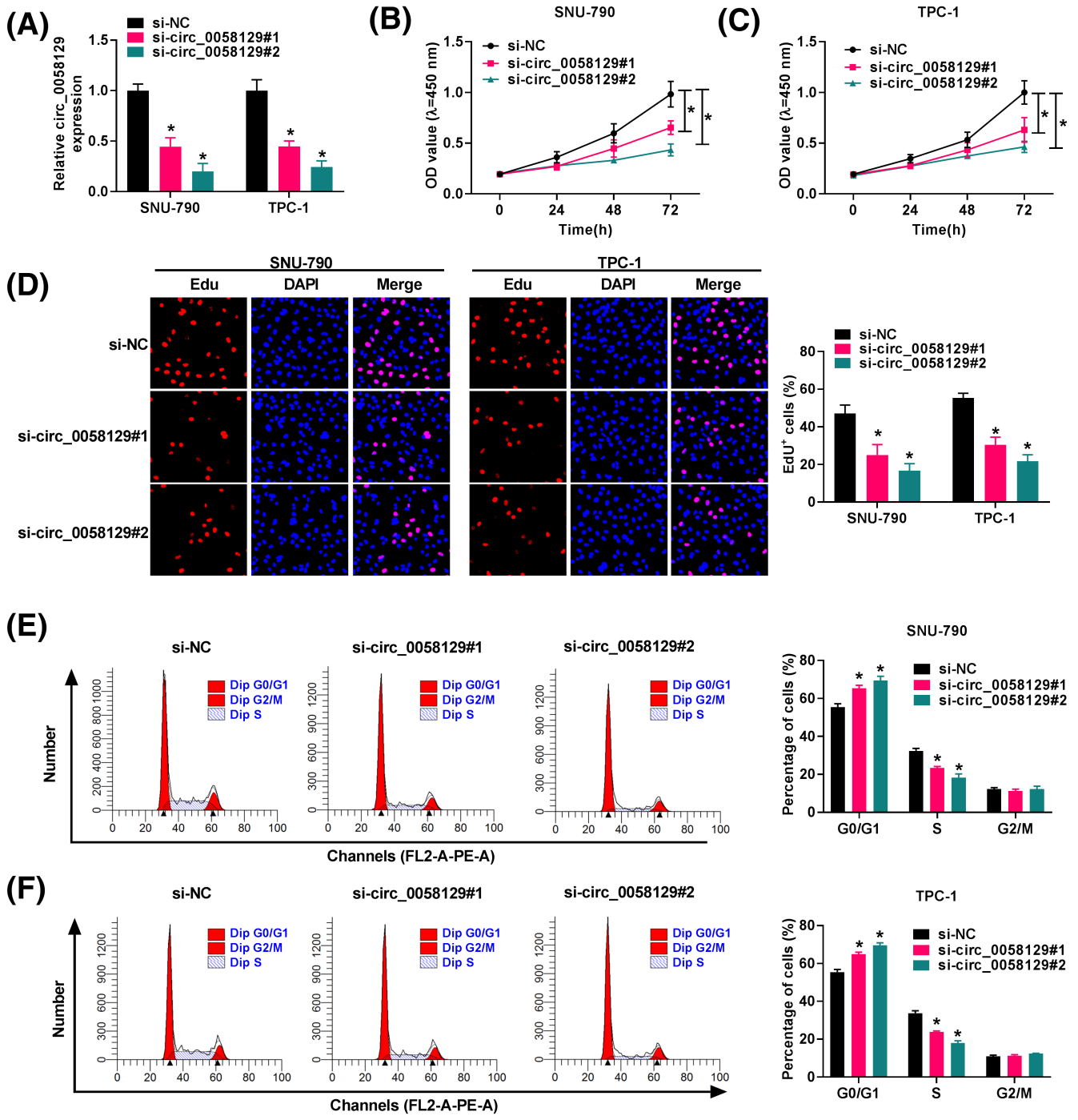

FIGURE 2 Circ_0058129 knockdown inhibited PTC progression. SUN-790 and TPC-1 cells were transfected with si-NC, si-circ_0058129#1, or si-circ_0058129#2. (A) The circ_0058129 content was measured by qRT-PCR. (B–D) The cell proliferation and (E and F) cell mitotic cycle were examined by CCK-8, EdU, and flow cytometry analysis. *$p < 0.05$

wild-type and mutant hsa_circ_0058129 or FSTL1 were manufactured by Ribobio Co., Ltd. with the use of pmirGLO vector (Promega), named as circ_0058129-WT, FSTL1 3'UTR-WT, circ_0058129-MUT, and FSTL1 3'UTR-MUT. At last, luciferase activity was quantified.

2.11 | RIP assay

A Magna RIP kit (Sigma) was utilized to implement RIP assay according to the previous method.[23] qRT-PCR was implemented to validate the contents of miR-873-5p, circ_0058129, and FSTL1.

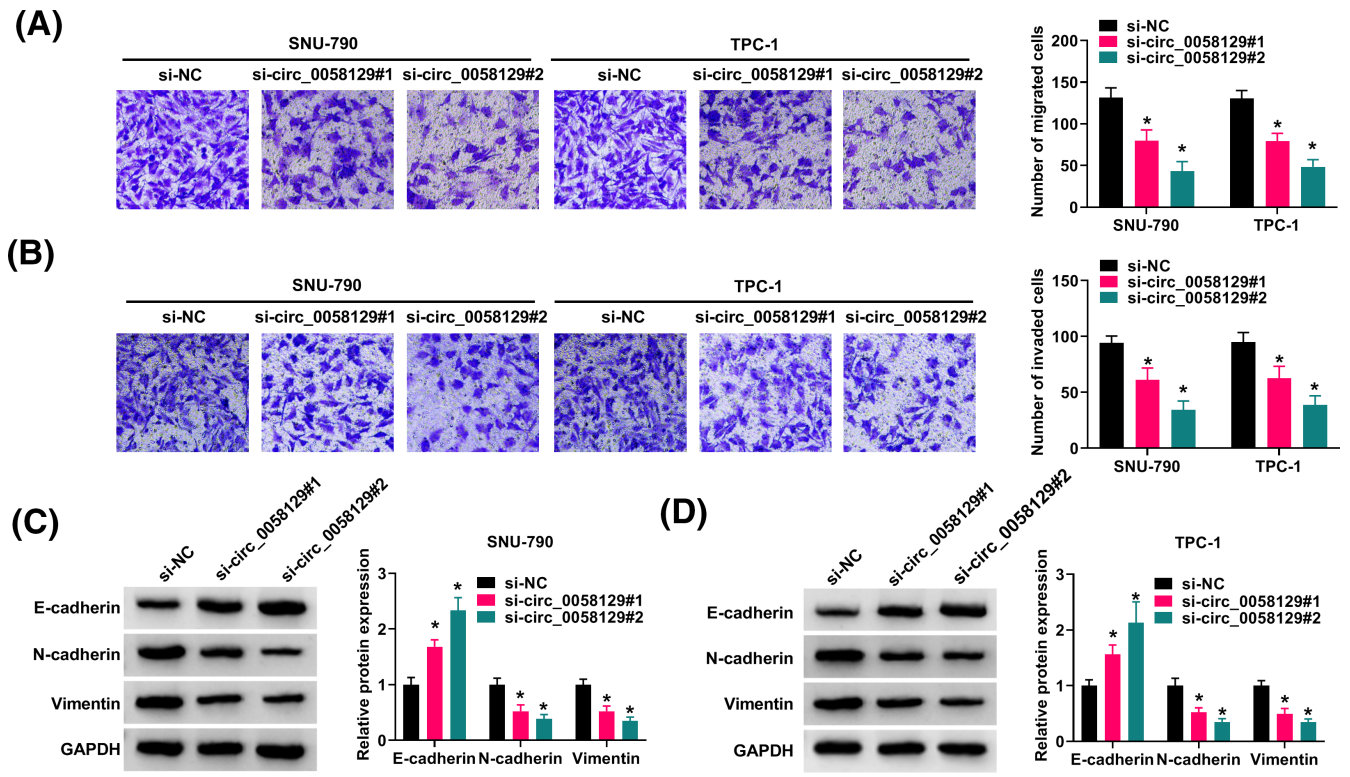

FIGURE 3 Circ_0058129 absence subdued PTC progression. SUN-790 and TPC-1 cells were transfected with si-NC, si-circ_0058129#1, or si-circ_0058129#2. (A and B) Cell migration and invasion were analyzed by transwell assay. (C and D) The abundances of E-cadherin, N-cadherin, and Vimentin were checked by western blot analysis. $^*p < 0.05$

2.12 | RNA pull-down assay

Biotinylated miR-873-5p (bio-miR-873-5p) and bio-miR-NC were provided by Sangon. SNU-790 and TPC-1 cells were transfected with bio-miR-873-5p and bio-miR-NC and cultured for 48 h. The cells were incubated in a specific lysis buffer for 10 min and then incubated with streptavidin-coupled beads (Invitrogen) for 4 h. At last, qRT-PCR was used to analyze circ_0058129 enrichment.

2.13 | Xenograft models

The animal assay was approved by the Animal Care and Use Committee of the Cancer Hospital of the University of Chinese Academy of Sciences. All mice were purchased from Beijing Vital River Laboratory Animal Technology Co., Ltd. TPC-1 cells with sh-circ_0058129 or sh-NC were injected into the mice (age: 6 weeks, weight: 18–22 g, $n = 6$/group). The volume of the forming tumors was measured according to the formula that volume = length × width^2 × 0.5. After 27 days, the tumor materials were harvested for further investigation.

2.14 | IHC assay

The tumor sections were exposed to 4% paraformaldehyde (Sigma) and embedded into paraffin. These slices were incubated with anti-FSTL1, anti-E-cadherin (ab40772; 1:10,000; Abcam), anti-N-cadherin (ab76011; 1:1,000; Abcam), and anti-Vimentin (ab92547; 1:1,000; Abcam), followed by incubating with a secondary antibody (ab150113, Abcam) for 1 h. These sections were stained with a DAB kit (Sigma). Results were analyzed according to the percentage of stained cells and intensity of immunostaining as instructed.[24]

2.15 | Statistical assay

All data were obtained from at least three independent duplicate tests. The difference was analyzed by Pearson's correlation analysis, Student's *t* test, or ANOVA using GraphPad Prism 7. $p < 0.05$ was considered statistically significant.

3 | RESULTS

3.1 | Circ_0058129 content was augmented in PTC

Firstly, circ_0058129 was located on chr2:216271849–216296687 and consists of exons 4–18 of the FN1 gene (Figure 1A). Circ_0058129 abundance was augmented in PTC tissues ($n = 70$) and cells (Figure 1B,C) compared with the controls. As displayed in Figure 1D,E, the FN1 mRNA level was abridged by RNase R, although circ_0058129 was not altered. Additionally, we found that circ_0058129 was mainly located in the cytoplasm of SNU-790 and TPC-1 cells (Figure 1F,G).

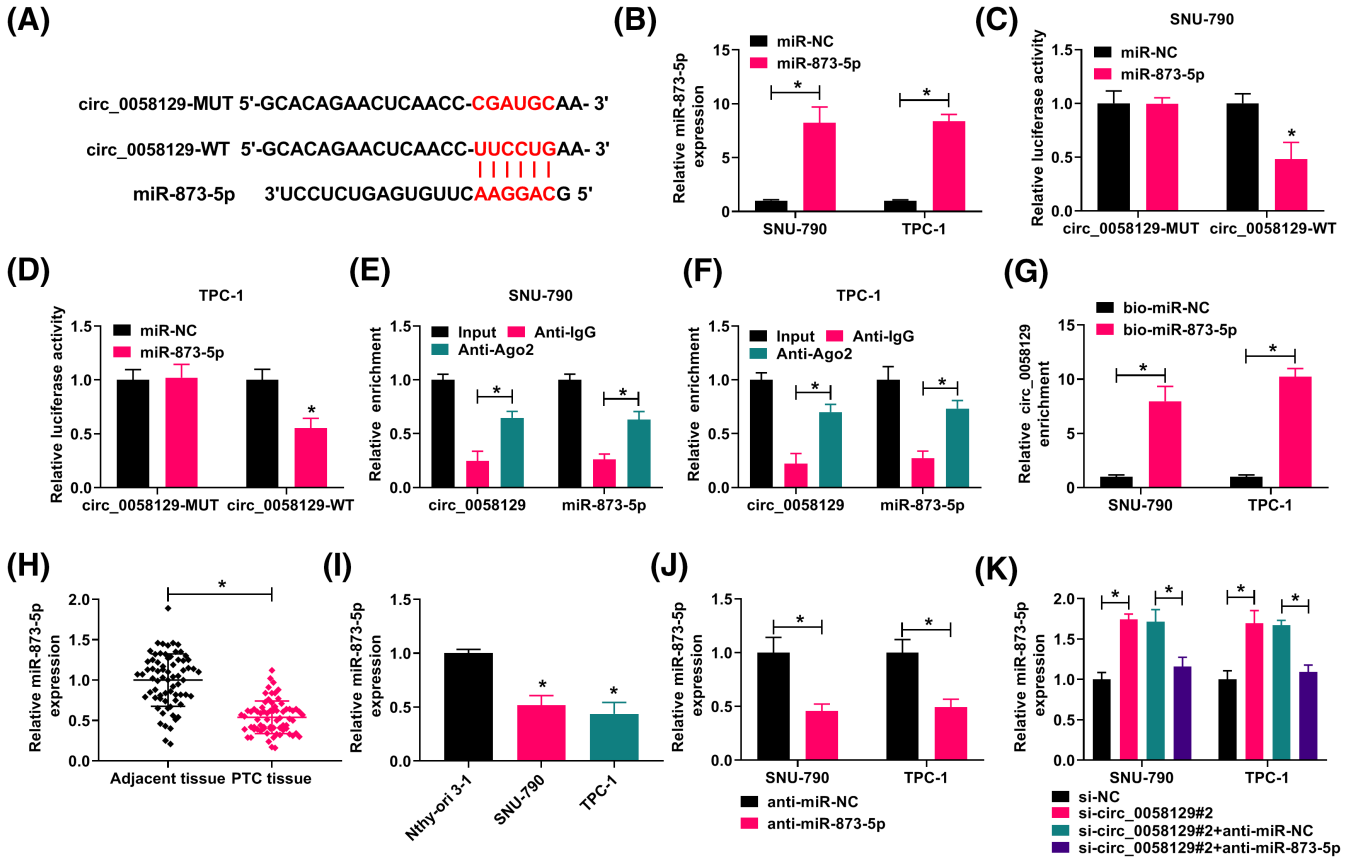

FIGURE 4 Circ_0058129 sponged miR-873-5p. (A) Circ_0058129-associated miRNAs were identified by circinteractome. (B) The content of miR-873-5p was detected by qRT-PCR after transfection of miR-873-5p or miR-NC. (C–G) The binding relationship of circ_0058129 and miR-873-5p was identified by dual-luciferase reporter, RIP, and RNA pull-down assays. (H and I) The content of miR-873-5p was examined by qRT-PCR in PTC tissues, normal tissues, Nthy-ori3-1 cells, SNU-790 cells, and TPC-1 cells. (J) The efficiency of miR-873-5p depletion was determined by qRT-PCR. (K) The effects of circ_0058129 knockdown and miR-873-5p depletion on miR-873-5p expression were analyzed by qRT-PCR. $^*p < 0.05$

The results demonstrated that circ_0058129 might be involved in PTC progression.

3.2 | Circ_0058129 absence repressed the development of PTC cells

Circ_0058129 abundance was reduced in PTC cells by si-circ_0058129#1 and si-circ_0058129#2 (Figure 2A). Moreover, circ_0058129 absence reduced cell proliferation (Figure 2B–D). In addition, si-circ_0058129#1 and si-circ_0058129#2 induced PTC cell arrest at the G0/G1 phase (Figure 2E,F). Subsequently, circ_0058129 absence repressed migration and invasion of PTC cells (Figure 3A,B). E-cadherin, N-cadherin, and Vimentin were key factors related to cell migration and invasion. Herein, si-circ_0058129#1 and si-circ_0058129#2 transfection conspicuously abridged the N-cadherin and Vimentin contents but enlarged E-cadherin in SNU-790 and TPC-1 cells (Figure 3C,D). Among them, si-circ_0058129#2 had a stronger effect on the process of cells, so it was selected for subsequent tests.

3.3 | MiR-873-5p bound to circ_0058129

As shown in Figure 4A, miR-873-5p potentially bound to circ_0058129. The abundance of miR-873-5p was boosted by miR-873-5p mimic (Figure 4B), showing the high efficiency of miR-873-5p overexpression. The luciferase activity was inhibited in circ_0058129-WT and miR-873-5p group in PTC cells versus the miR-NC groups (Figure 4C,D). Besides, the RIP assay uncovered the binding relationship of miR-873-5p and circ_0058129 in TPC-1 and SNU-790 cells (Figure 4E,F). As shown in Figure 4G, bio-miR-873-5p dramatically enriched circ_0058129 compared with the bio-miR-NC group. Furthermore, miR-873-5p content was reduced in PTC tumor tissues ($n = 70$) and cells (TPC-1 and SNU-790) compared with the control groups (Figure 4H,I). The abundance of miR-873-5p was reduced by anti-miR-873-5p (Figure 4J), suggesting the success of miR-873-5p knockdown. Moreover, miR-873-5p was amplified by si-circ_0058129#2, but it was declined by anti-miR-873-5p (Figure 4K). These data demonstrated that circ_0058129 bound to miR-873-5p.

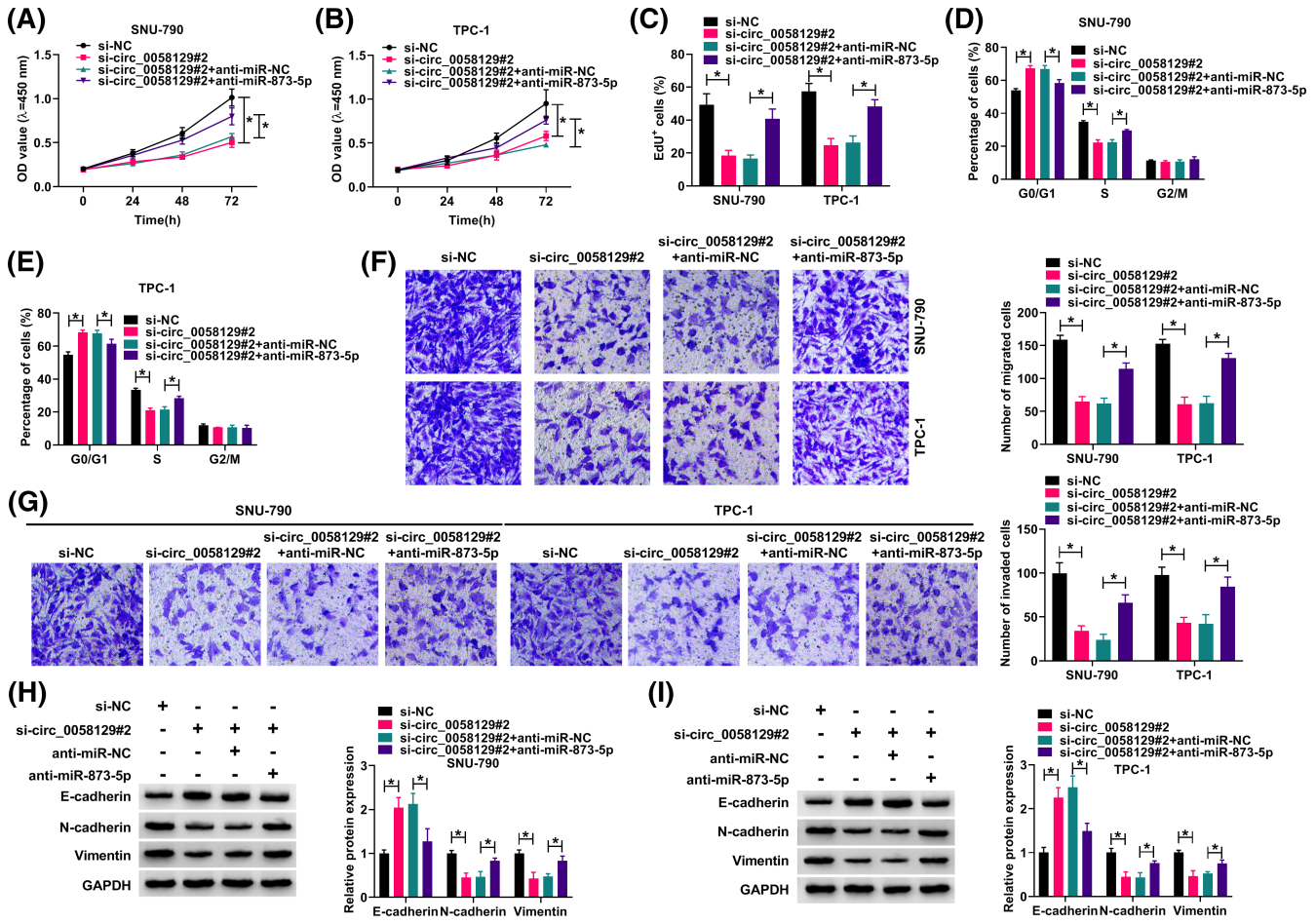

FIGURE 5 Circ_0058129 expedited PTC via miR-873-5p. SUN-790 and TPC-1 cells were transfected with si-NC, si-circ_0058129#2, anti-miR-NC, and anti-miR-873-5p alone or jointly. (A–E) Cell proliferation was analyzed by CCK-8, EdU, and flow cytometry analysis. (F and G) Cell migration and invasion were investigated by transwell assays. (H and I) The abundances of E-cadherin, N-cadherin, and Vimentin were examined by western blot. $^*p < 0.05$

3.4 | Circ_0058129 knockdown repressed PTC cell processes via miR-873-5p

Firstly, circ_0058129 absence weakened the cell proliferation, whereas this influence was lessened by anti-miR-873-5p (Figure 5A–C). In addition, si-circ_0058129#2 induced PTC cell arrest at the G0/G1 phase, but this effect was remitted by anti-miR-873-5p (Figure 5D,E). The absence of circ_0058129 weakened the cell migration and invasion; nevertheless, these impacts were diminished by anti-miR-873-5p (Figure 5F,G). Furthermore, anti-miR-873-5p reserved circ_0058129 absence-induced dysregulation on N-cadherin, Vimentin, and E-cadherin in PTC cells (Figure 5H,I). Thus, these findings explained the circ_0058129/miR-873-5p axis regulated PTC cell malignancy.

3.5 | MiR-873-5p targeted FSTL1 in PTC cells

The binding sites of miR-873-5p in FSTL1 3'UTR were shown in Figure 6A. The luciferase activity of FSTL1 3'UTR-WT was hampered by miR-873-5p, but there was no alteration in the luciferase activity of FSTL1 3'UTR-MUT and miR-873-5p group (Figure 6B,C). The RIP assay uncovered the association of miR-873-5p and FSTL1 in TPC-1 and SNU-790 cells (Figure 6D,E). Furthermore, FSTL1 level was boosted in PTC tumor tissues and cells (Figure 6F–H). FSTL1 abundance was improved after FSTL1 transfection (Figure 6I). Besides, FSTL1 was restrained by miR-873-5p upregulation, whereas the effect was attenuated by increasing FSTL1 expression (Figure 6J). Therefore, all data manifested that miR-873-5p targeted FSTL1.

3.6 | MiR-873-5p inhibited PTC cell malignancy through FSTL1

MiR-873-5p curbed SNU-790 and TPC-1 cell proliferation, but this effect was abolished by FSTL1 (Figure 7A–C). The miR-873-5p mimics induced PTC cell arrest at the G0/G1 phase, while this effect was rescued after FSTL1 overexpression (Figure 7D,E). Moreover, miR-873-5p weakened the cell migration and invasion; nevertheless, these consequences were restored when FSTL1 expression

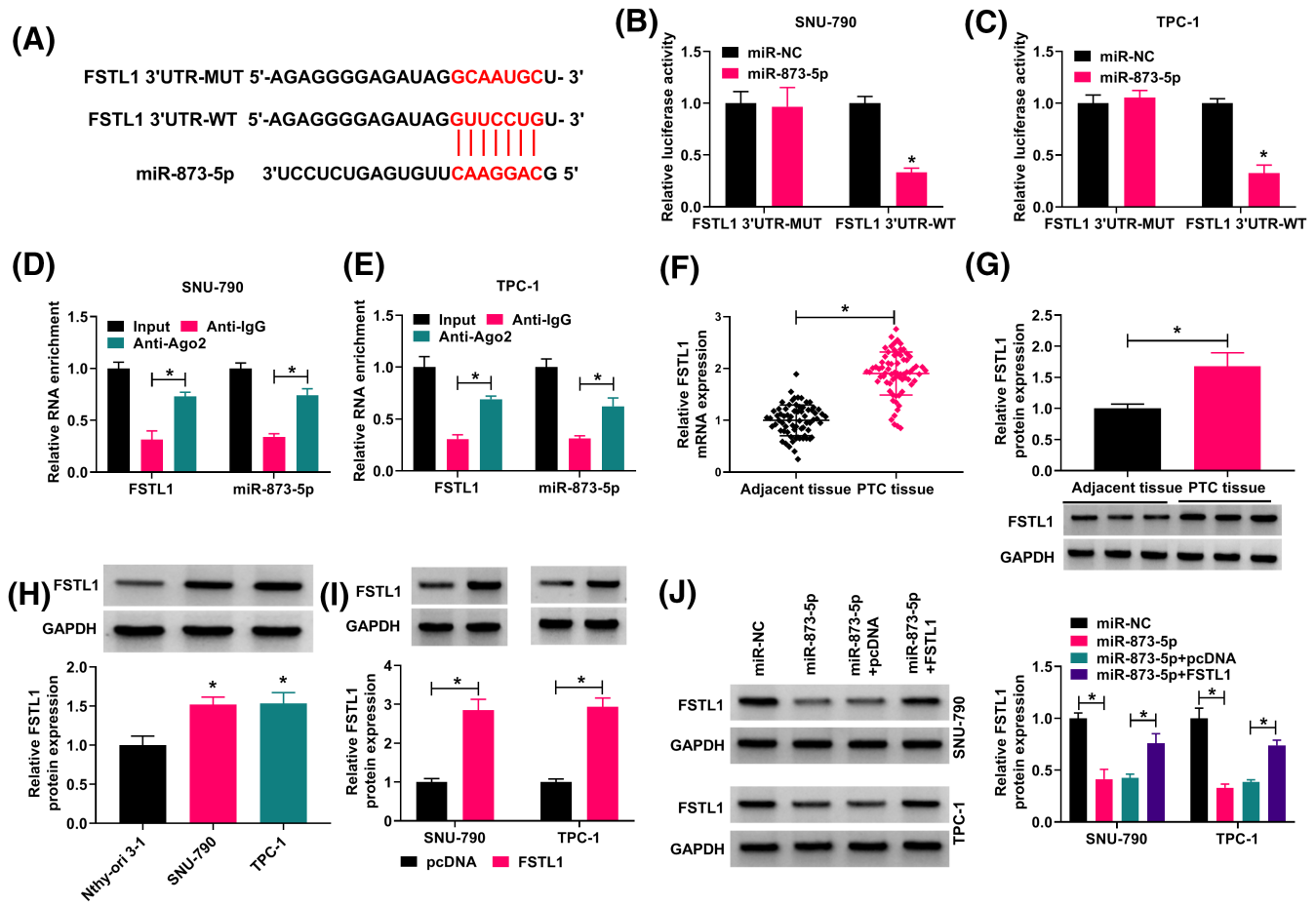

FIGURE 6 MiR-873-5p targeted FSTL1. (A) The schematic illustration showed the combinative sites of miR-873-5p and FSTL1. (B–E) The association of miR-873-5p and FSTL1 was analyzed by dual-luciferase reporter assay and RIP assay. (F–H) The content of FSTL1 was detected by qRT-PCR and western blot analysis in PTC tissues, normal tissues, Nthy-ori3-1 cells, SNU-790 cells, and TPC-1 cells. (I and J) The abundances of miR-873-5p and FSTL1 in PTC cells were detected by western blot. $^*p < 0.05$

was increased (Figure 7F,G). Besides, FSTL1 curbed the influences of miR-873-5p on N-cadherin, Vimentin, and E-cadherin levels in PTC cells (Figure 7H,I). Taken together, these data demonstrated that the miR-873-5p/FSTL1 pathway regulated PTC cell malignancy.

3.7 | FSTL1 was adjusted by the circ_0058129/miR-873-5p pathway

Follistatin-like 1 level was weakened by si-circ_0058129#2, while anti-miR-873-5p diminished the effect (Figure 8A). Moreover, miR-873-5p was negatively correlated with circ_0058129 (Figure 8B) and FSTL1 (Figure 8C) in PTC tissues. In addition, circ_0058129 was positively correlated with FSTL1 in PTC tissues (Figure 8D).

3.8 | Circ_0058129 absence impeded tumor growth in vivo

As shown in Figure 9A–C, the sh-circ_0058129 repressed tumor volume and weight. Furthermore, the abundances of circ_0058129 and FSTL1 were decreased, although the miR-873-5p level was increased in the sh-circ_0058129 group compared with the sh-NC group (Figure 9D–F). IHC assay showed that the FSTL1, N-cadherin, and Vimentin contents were lower, but E-cadherin was higher in the sh-circ_0058129 group than in the sh-NC group (Figure 9G). These consequences pointed out that circ_0058129 absence repressed xenograft tumor growth via miR-873-5p/FSTL1 axis in vivo.

4 | DISCUSSION

Currently, the therapeutic approach of PTC includes surgery and radioactive iodine therapy.[25,26] Although the majority of PTC patients have a good prognosis, some patients are still stuck owing to tumor recurrence and metastasis.[27] Meanwhile, there is no effective treatment for locally advanced or severely metastatic PTC patients.[28] As reported, there were many differentially expressed circRNAs in PTC tissues. Herein, our research revealed the role of circ_0058129 in PTC progression.

Some circRNAs were vital for PTC progression. For example, Ding et al. reported that high expression of hsa_circ_0015278

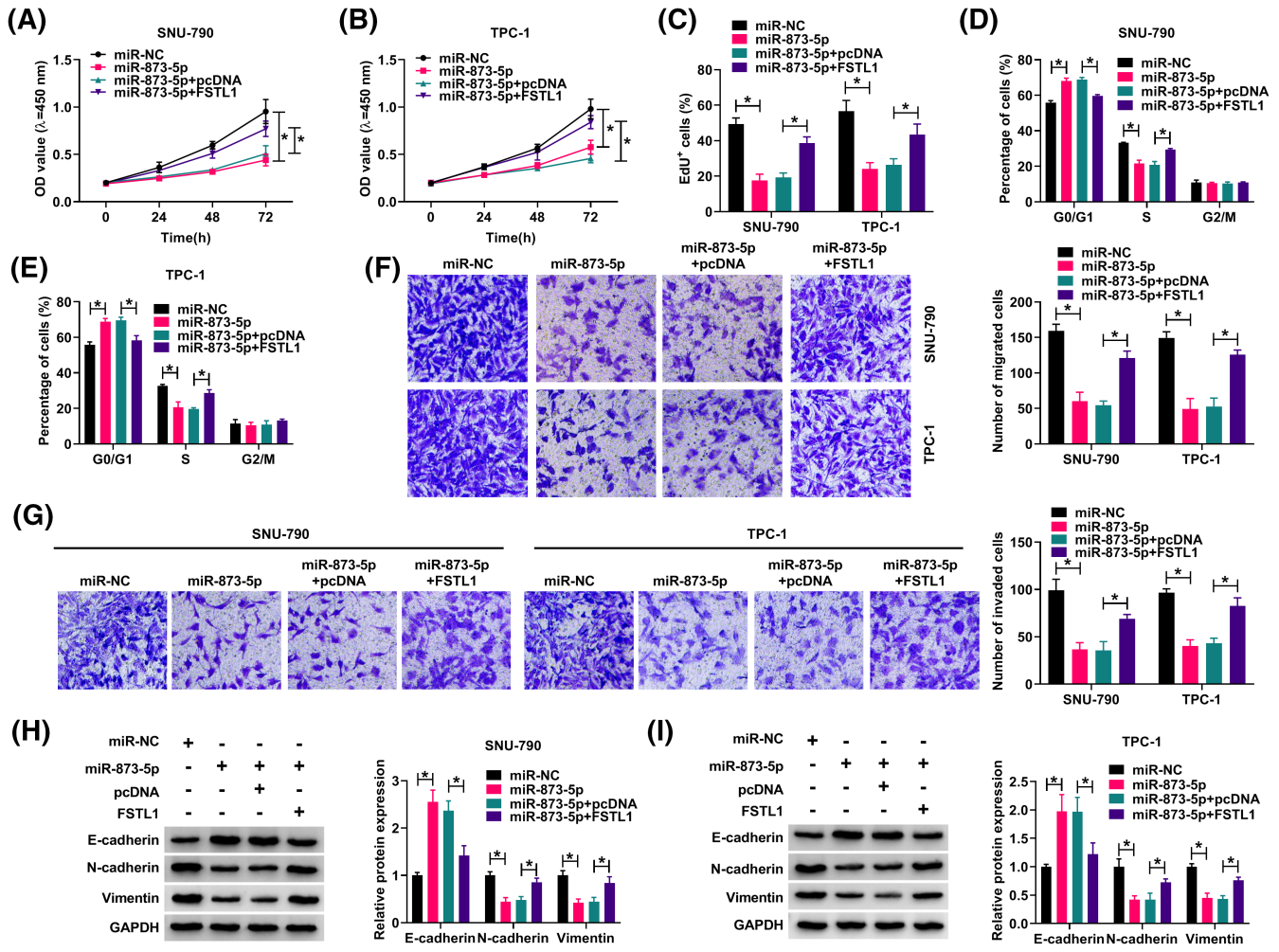

FIGURE 7 MiR-873-5p adjusted PTC via FSTL1. SUN-790 and TPC-1 cells were transfected with miR-NC, miR-873-5p, miR-873-5p, and FSTL1 alone or jointly. (A–E) Cell proliferation was analyzed by CCK-8, EdU, and flow cytometry analysis. (F and G) Cell migration and invasion were investigated by transwell assays. (H and I) The abundances of E-cadherin, N-cadherin, and Vimentin were examined by western blot. $^*p < 0.05$

was associated with extrathyroidal invasion, pathological node stage, and reduced relapse rate.[29] Hsa_circ_102002 facilitated PTC cell migration and epithelial–mesenchymal transition.[30] Hsa_circ_0025033 contributed to PTC cell proliferation in vitro and in vivo.[31] Our results showed that the circ_0058129 absence inhibited the proliferation, migration, and invasion of PTC cells for the first time. Furthermore, our in vivo study discovered that knockdown of circ_0058129 impaired tumor growth. There has been growing information uncover that circRNAs influence cancer development by binding to miRNAs. For example, hsa_circ_102002 targeted miR-488-3p and hsa_circ_0025033 combined with miR-1179 to modulate PTC cell malignancy.[30,31] Herein, we found that circ_0058129 promoted PTC development by regulating miR-873-5p.

MiR-873-5p participated in the progression of triple-negative breast cancer (TNBC), glioma, and gastric carcinoma.[32–34] MiR-873-5p curbed papillary thyroid cancer cell invasion by interfering C-X-C motif chemokine ligand 16 (CXCL16).[14] MiR-873-5p regulated cell growth and metastasis in TNBC via MYC proto-oncogene, bHLH transcription factor (MYC).[32] In addition, miR-873-5p curbed cell growth and stimulated cell apoptosis in glioma cells through zinc finger E-box binding homeobox 2 (ZEB2).[35] Moreover, miR-873-5p regulated gastric cancer advancement via SEC11 homolog A, signal peptidase complex subunit (SPC18).[36] These results revealed that miR-873-5p was important to cancer development. Herein, we reported that miR-873-5p controlled the advancement of PTC. We also uncovered miR-873-5p inhibited cell growth through interaction with FSTL1. These data corroborated that miR-873-5p played a key part in the advancement of PTC.

Follistatin-like 1 played a vital character in the temozolomide resistance of glioblastoma.[37] Moreover, FSTL1 could regulate immune cell infiltration in gastric cancer.[38] FSTL1 enhanced chemoresistance in breast cancer cells.[39] FSTL1 could stimulate colorectal cancer cell metastasis.[40] In addition, FSTL1 reduced the cisplatin resistance of epithelial ovarian cancer.[41] In this work, FSTL1 was boosted in PTC tissues and cells. MiR-873-5p blocked cell growth, and this influence was diminished by FSTL1. We also explained that

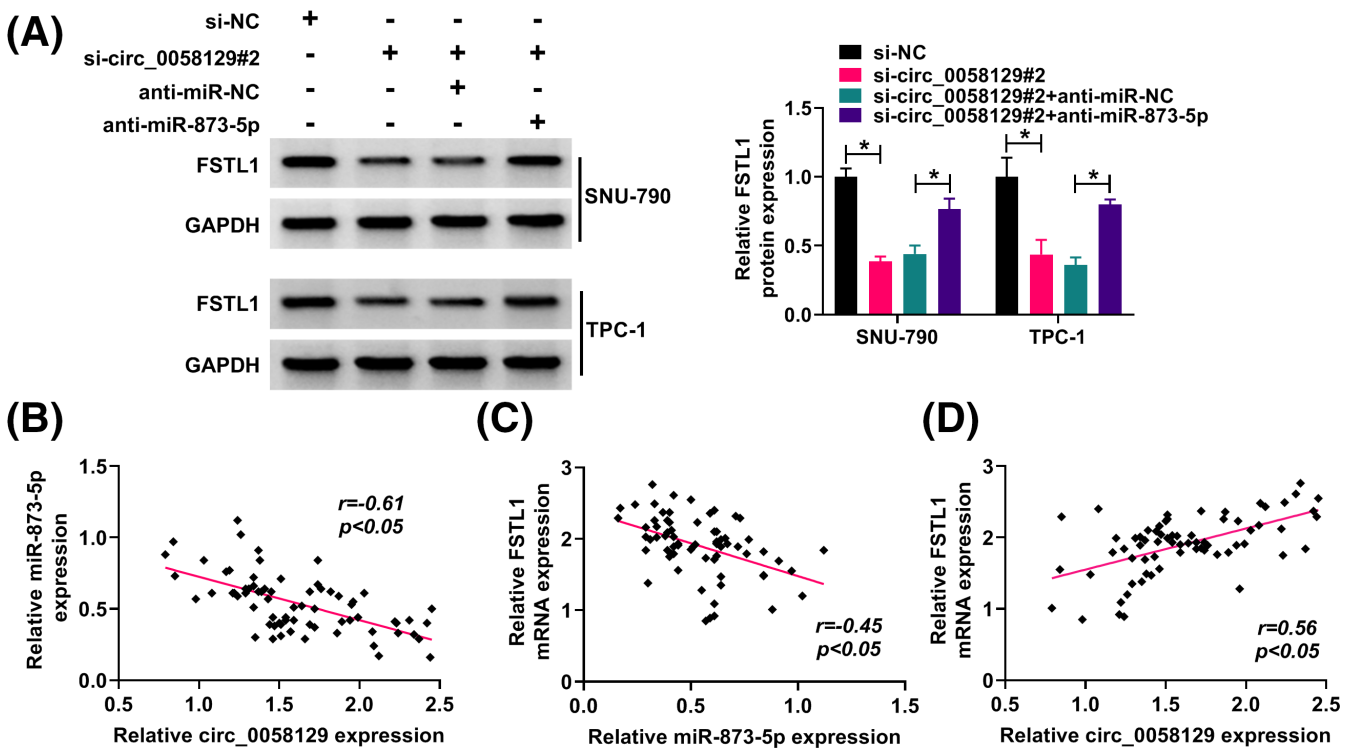

FIGURE 8 Follistatin-like 1 content was adjusted by circ_0058129 and miR-873-5p. (A) The abundance of FSTL1 was quantified by western blot. (B) Circ_0058129 was negatively correlated with miR-873-5p ($R = -0.63$) in PTC tissues. (C) FSTL1 was negatively correlated with miR-873-5p ($R = -0.49$) in PTC tissues. (D) FSTL1 was positively correlated with circ_0058129 ($R = 0.58$) in PTC tissues. *$p < 0.05$

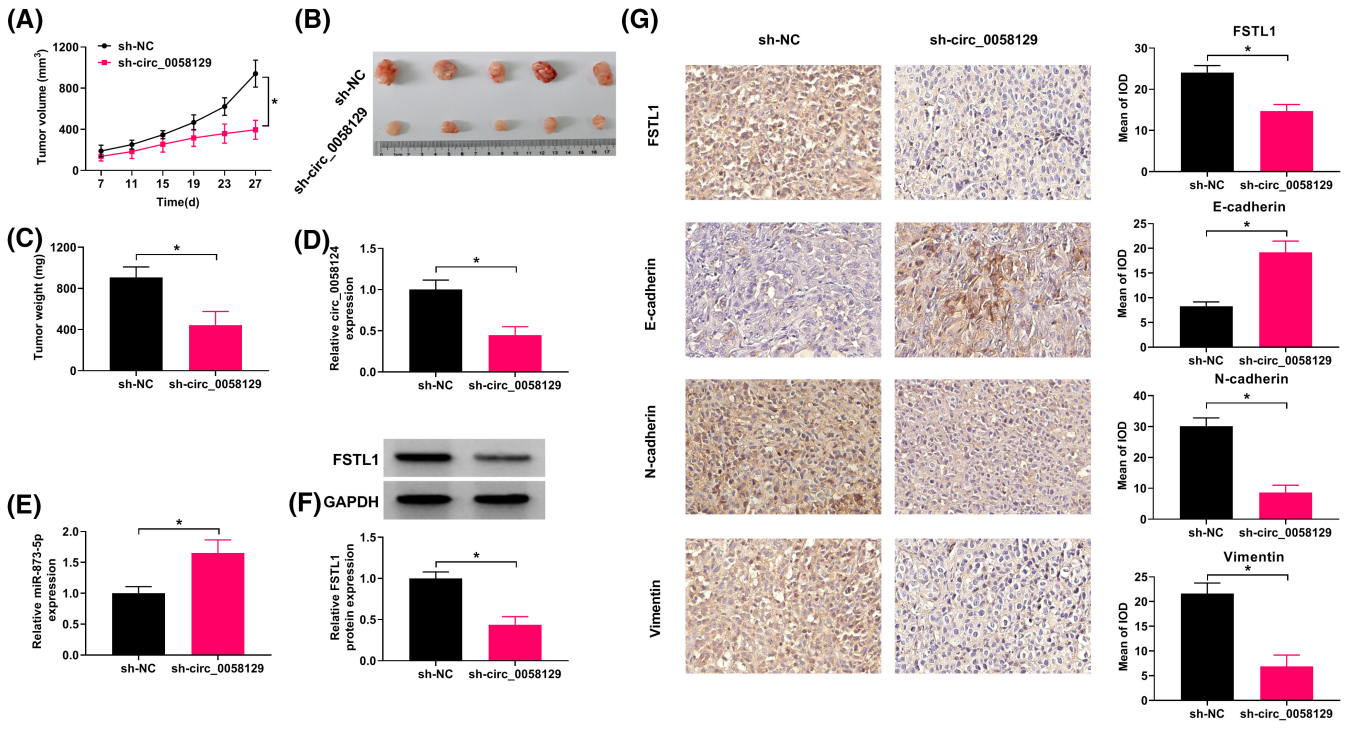

FIGURE 9 Circ_0058129 knockdown diminished tumor growth. (A–C) Tumor growth was detected. (D–F) The circ_0058129, miR-873-5p, and FSTL1 contents were quantified by qRT-PCR or western blot in the forming tumor tissues from sh-circ_0058129 or sh-NC group. (G) The FSTL1, E-cadherin, N-cadherin, and Vimentin levels were detected by IHC assay in the primary tumors from TPC-1. *$p < 0.05$

miR-873-5p depletion rescued the effect of circ_0058129 absence on FSTL1 level in PTC cells.

In brief, the research demonstrated that circ_0058129 and FSTL1 contents were increased and miR-873-5p level was decreased in PTC tissues and cells. Additionally, our study uncovered that circ_0058129 absence inhibited cell proliferation, migration and invasion in PTC cells via miR-873-5p/FSTL1 axis. This regulatory network needed to be corroborated by clinical assays in the future. These data might provide innovative ideas for PTC management.

ACKNOWLEDGEMENT

None.

CONFLICT OF INTEREST

The authors declare that they have no conflicts of interest.

ORCID

Xiangrong Tan https://orcid.org/0000-0001-8779-7988

REFERENCES

1. Zhu X, Yao J, Tian W. Microarray technology to investigate genes associated with papillary thyroid carcinoma. *Mol Med Rep*. 2015;11:3729-3733.
2. LiVolsi VA. Papillary thyroid carcinoma: an update. *Mod Pathol*. 2011;24(Suppl 2):S1-S9.
3. Grogan RH, Kaplan SP, Cao H, et al. A study of recurrence and death from papillary thyroid cancer with 27 years of median follow-up. *Surgery*. 2013;154:1436-1446; Discussion 1446–1437.
4. Greene J, Baird AM, Brady L, et al. Circular RNAs: biogenesis, function and role in human diseases. *Front Mol Biosci*. 2017;4:38.
5. Sheng JQ, Liu L, Wang MR, Li PY. Circular RNAs in digestive system cancer: potential biomarkers and therapeutic targets. *Am J Cancer Res*. 2018;8:1142-1156.
6. Bi W, Huang J, Nie C, et al. CircRNA circRNA_102171 promotes papillary thyroid cancer progression through modulating CTNNBIP1-dependent activation of beta-catenin pathway. *J Exp Clin Cancer Res*. 2018;37:275.
7. Ma J, Kan Z. Circ_0137287 suppresses cell tumorigenesis and aerobic glycolysis in papillary thyroid carcinoma through miR-183-5p/PPP2R2A axis. *Cytotechnology*. 2021;73:497-511.
8. Wu G, Zhou W, Pan X, et al. Circular RNA profiling reveals exosomal circ_0006156 as a novel biomarker in papillary thyroid cancer. *Mol Ther Nucleic Acids*. 2020;19:1134-1144.
9. Yao Y, Chen X, Yang H, et al. Hsa_circ_0058124 promotes papillary thyroid cancer tumorigenesis and invasiveness through the NOTCH3/GATAD2A axis. *J Exp Clin Cancer Res*. 2019;38:318.
10. Geng QS, Huang T, Li LF, Shen ZB, Xue WH, Zhao J. Overexpression and prognostic significance of FN1, correlating with immune infiltrates in thyroid cancer. *Front Med (Lausanne)*. 2021;8:812278.
11. Ambros V. The functions of animal microRNAs. *Nature*. 2004;431:350-355.
12. Garzon R, Marcucci G, Croce CM. Targeting microRNAs in cancer: rationale, strategies and challenges. *Nat Rev Drug Discov*. 2010;9:775-789.
13. Zhu Y, Zhang X, Qi M, Zhang Y, Ding F. miR-873-5p inhibits the progression of colon cancer via repression of tumor suppressor candidate 3/AKT signaling. *J Gastroenterol Hepatol*. 2019;34:2126-2134.
14. Wang Z, Liu W, Wang C, Ai Z. miR-873-5p inhibits cell migration and invasion of papillary thyroid cancer via regulation of CXCL16. *Onco Targets Ther*. 2020;13:1037-1046.
15. Cao D, Yu T, Ou X. MiR-873-5P controls gastric cancer progression by targeting hedgehog-GLI signaling. *Pharmazie*. 2016;71:603-606.
16. Lei H, Gao Y, Xu X. LncRNA TUG1 influences papillary thyroid cancer cell proliferation, migration and EMT formation through targeting miR-145. *Acta Biochim Biophys Sin (Shanghai)*. 2017;49:588-597.
17. Xu Y, Han YF, Zhu SJ, Dong JD, Ye B. miRNA148a inhibits cell growth of papillary thyroid cancer through STAT3 and PI3K/AKT signaling pathways. *Oncol Rep*. 2017;38:3085-3093.
18. Chaly Y, Hostager B, Smith S, Hirsch R. Follistatin-like protein 1 and its role in inflammation and inflammatory diseases. *Immunol Res*. 2014;59:266-272.
19. Sylva M, Li VS, Buffing AA, et al. The BMP antagonist follistatin-like 1 is required for skeletal and lung organogenesis. *PLoS One*. 2011;6:e22616.
20. Yang Y, Liu J, Mao H, Hu YA, Yan Y, Zhao C. The expression pattern of Follistatin-like 1 in mouse central nervous system development. *Gene Expr Patterns*. 2009;9:532-540.
21. Sylva M, Moorman AF, van den Hoff MJ. Follistatin-like 1 in vertebrate development. *Birth Defects Res C Embryo Today*. 2013;99:61-69.
22. Ni X, Cao X, Wu Y, Wu J. FSTL1 suppresses tumor cell proliferation, invasion and survival in non-small cell lung cancer. *Oncol Rep*. 2018;39:13-20.
23. Bian W, Jing X, Yang Z, et al. Downregulation of LncRNA NORAD promotes Ox-LDL-induced vascular endothelial cell injury and atherosclerosis. *Aging (Albany NY)*. 2020;12:6385-6400.
24. Huang D-W, Huang M, Lin X-S, Huang Q. CD155 expression and its correlation with clinicopathologic characteristics, angiogenesis, and prognosis in human cholangiocarcinoma. *Onco Targets Ther*. 2017;10:3817-3825.
25. Jillard CL, Scheri RP, Sosa JA. What is the optimal treatment of papillary thyroid cancer? *Adv Surg*. 2015;49:79-93.
26. McLeod DS, Sawka AM, Cooper DS. Controversies in primary treatment of low-risk papillary thyroid cancer. *Lancet*. 2013;381:1046-1057.
27. Lonjou C, Damiola F, Moissonnier M, et al. Investigation of DNA repair-related SNPs underlying susceptibility to papillary thyroid carcinoma reveals MGMT as a novel candidate gene in Belarusian children exposed to radiation. *BMC Cancer*. 2017;17:328.
28. Brennan K, Holsinger C, Dosiou C, et al. Development of prognostic signatures for intermediate-risk papillary thyroid cancer. *BMC Cancer*. 2016;16:736.
29. Ding H, Wang X, Liu H, Na L. Higher circular RNA_0015278 correlates with absence of extrathyroidal invasion, lower pathological tumor stages, and prolonged disease-free survival in papillary thyroid carcinoma patients. *J Clin Lab Anal*. 2021;35:e23819.
30. Zhang W, Liu T, Li T, Zhao X. Hsa_circRNA_102002 facilitates metastasis of papillary thyroid cancer through regulating miR-488-3p/HAS2 axis. *Cancer Gene Ther*. 2021;28:279-293.
31. Ye M, Hou H, Shen M, Dong S, Zhang T. Circular RNA circFOXM1 plays a role in papillary thyroid carcinoma by sponging miR-1179 and regulating HMGB1 expression. *Mol Ther Nucleic Acids*. 2020;19:741-750.
32. Tang L, Chen Y, Tang X, Wei D, Xu X, Yan F. Long noncoding RNA DCST1-AS1 promotes cell proliferation and metastasis in triple-negative breast cancer by forming a positive regulatory loop with miR-873-5p and MYC. *J Cancer*. 2020;11:311-323.
33. Lin Y-H, Guo L, Yan F, Dou Z-Q, Yu Q, Chen G. Long non-coding RNA HOTAIRM1 promotes proliferation and inhibits apoptosis of glioma cells by regulating the miR-873-5p/ZEB2 axis. *Chin Med J (Engl)*. 2020;133:174-182.
34. Ma Y, Xu XL, Huang HG, Li YF, Li ZG. LncRNA TDRG1 promotes the aggressiveness of gastric carcinoma through regulating miR-873-5p/HDGF axis. *Biomed Pharmacother*. 2020;121:109425.

35. Corrigendum: long non-coding RNA HOTAIRM1 promotes proliferation and inhibits apoptosis of glioma cells by regulating the miR-873-5p/ZEB2 axis. *Chin Med J (Engl)*. 2020;133:1007.
36. Ren Z, Liu X, Si Y, Yang D. Long non-coding RNA DDX11-AS1 facilitates gastric cancer progression by regulating miR-873-5p/SPC18 axis. *Artif Cells Nanomed Biotechnol*. 2020;48:572-583.
37. Nie E, Miao F, Jin X, et al. Fstl1/DIP2A/MGMT signaling pathway plays important roles in temozolomide resistance in glioblastoma. *Oncogene*. 2019;38:2706-2721.
38. Li L, Huang S, Yao Y, et al. Follistatin-Like 1 (FSTL1) is a prognostic biomarker and correlated with immune cell infiltration in gastric cancer. *World J Surg Oncol*. 2020;18:324.
39. Cheng S, Huang Y, Lou C, He Y, Zhang Y, Zhang Q. FSTL1 enhances chemoresistance and maintains stemness in breast cancer cells via integrin beta3/Wnt signaling under miR-137 regulation. *Cancer Biol Ther*. 2019;20:328-337.
40. Gu C, Wang X, Long T, et al. FSTL1 interacts with VIM and promotes colorectal cancer metastasis via activating the focal adhesion signalling pathway. *Cell Death Dis*. 2018;9:654.
41. Liu YK, Jia YJ, Liu SH, Ma J. FSTL1 increases cisplatin sensitivity in epithelial ovarian cancer cells by inhibition of NF-kappaB pathway. *Cancer Chemother Pharmacol*. 2021;87:405-414.

How to cite this article: Tan X, Zhao J, Lou J, Zheng W, Wang P. Hsa_circ_0058129 regulates papillary thyroid cancer development via miR-873-5p/follistatin-like 1 axis. *J Clin Lab Anal*. 2022;36:e24401. doi:10.1002/jcla.24401